

Enhancing Food Security in Africa with a Predictive Early Warning System on Extreme Weather Phenomena

Alvin M Igobwa

iLab

Jeremy Gachanja

iLab

Betsy Muriithi

iLab

John Olukuru

iLab

Angeline Rehema Wairegi (✉ awairegi@strathmore.edu)

Strathmore University <https://orcid.org/0000-0002-7408-3502>

Isaac Rutenberg

CIPIT

Research Article

Keywords: Climate Change, Food Security, Extreme Weather Prediction, Agricultural Insurance, Insurance Based Index

Posted Date: March 2nd, 2022

DOI: <https://doi.org/10.21203/rs.3.rs-1343486/v1>

License: © ⓘ This work is licensed under a Creative Commons Attribution 4.0 International License.

[Read Full License](#)

1
2
3
4
5
6
7
8
9
10
11
12
13
14
15
16
17

Enhancing Food Security in Africa with a Predictive Early Warning System on
Extreme Weather Phenomena

Person A¹, Person B¹, Person C¹, Person D¹, Person E*², Person F²

Institution One ¹; Institution Two²

* Corresponding Author

person.a@institution.edu¹, person.b@institution.edu¹, person.c@institution.edu¹, person.d@institution.edu¹,
person.e@institution.edu², person.f@institution.edu².

18 Enhancing Food Security in Africa with a Predictive Early Warning System
19 on Extreme Weather Phenomena

20 Abstract

21 Climate change is predicted to exacerbate Africa's, already, precarious food security. Climate
22 models, by accurately forecasting future weather events, can be a critical tool in developing
23 countermeasures to reduce crop loss, decrease adverse effects on animal husbandry and fishing,
24 and even help insurance companies determine risk for agricultural insurance policies – a measure
25 of risk reduction in the agricultural sector that is gaining prominence. In this paper, we investigate
26 the efficacy of various open-source climate change models and weather datasets in predicting
27 drought and flood weather patterns in northern and western Kenya and discuss practical
28 applications of these tools in the country's agricultural insurance sector. We identified two models
29 that may be used to predict flood and drought events in these regions. The combination of Artificial
30 Neural Networks (ANNs) and weather station data was the most effective in predicting future
31 drought occurrences in Turkana and Wajir with accuracies ranging from 78% to 90%. In the case
32 of flood forecasting, Isolation Forests models using weather station data had the best overall
33 performance. The above models and datasets may form the basis of a more objective and accurate
34 underwriting process for agricultural index-based insurance, as we expound in the paper.

35 **Keywords:** Climate Change, Food Security, Extreme Weather Prediction, Agricultural Insurance,
36 Insurance Based Index

37 1. Introduction

38 Agriculture is the most important economic activity in Africa, accounting for 30% Gross Domestic
39 Product (GDP) across the continent (23% of Sub – Saharan Africa’s GDP) and employing 60% -
40 65% of the continent’s workforce (Goedde, Ooko - Ombaka and Pais 2019). While agricultural
41 production has increased steadily in Africa since the 1970s, there has been no significant
42 improvements in the production factors, i.e., labor and land; consequently, the sector’s growth has
43 been insufficient to adequately address poverty, attain food security, and lead to sustained GDP
44 growth on the continent (Bjornlund, Bjornlund and Van Rooyen 2018, Food and Agriculture
45 Organization (FAO) 2009, Pfister, et al. 2011). Climate change and a population boom have further
46 contributed to food insecurity.

47 The impact of climate change in Africa is predicted to be greater than anywhere else on the globe.
48 Sub-Saharan Africa is especially vulnerable to climate change due to a confluence of biophysical,
49 political, and socioeconomic stresses that interact to increase the region’s susceptibility and
50 constrain its adaptive capacity. Climate change in Sub-Saharan Africa is expected to manifest in
51 an increase in temperatures (an average increase of 3–4 °C over the next century, greater than the
52 projected global annual mean), changes in rainfall intensity, increase in extreme weather
53 phenomena such as droughts and flood, increase in desertification, and changes in the spatial and
54 temporal transmission of infectious diseases – events that are likely to cause disruptions in growing
55 seasons, reductions in the area suitable for agriculture, and declines in agricultural yield (Boko, et
56 al. 2007, Chen, et al. 2006, Muller, et al. 2011, Niang, et al. 2014, Reich, et al. 2001, Richard, et
57 al. 2001, Sarr 2012, Songok, Kipkorir and Mugalavai 2011, Thomas, et al. 2007). A majority of
58 its population is still dependent upon these local natural resources for their livelihood; engaging in
59 activities such as agriculture, pastoralism, and fishing for sustenance and revenue (Osahr, et al.
60 2008, Wlokas 2008). Climate change (experienced over longer time frames as changes in climatic
61 norms and over shorter periods as changes in the frequency and severity of extreme weather
62 events) impedes farmers’, pastoralists’, and agro-pastoralists’ ability to grow crops and rear
63 livestock, and, in general, has a negative impact on the livelihoods of communities, especially
64 those in rural areas (Connolly-Boutin and Smit 2016, Kebede, Hasen and Negatu 2011, Songok,
65 Kipkorir, et al. 2011, Thompson and Scoones 2009). Only 5% of farmlands in Africa are irrigated
66 compared to 37% in Asia and 14% in Latin America, making them more dependent on natural
67 precipitation (Ringler, et al. 2010).

68 Solutions to food insecurity have, in the past, largely focused on agricultural intensification as a
69 mechanism for greater crop production; farming diversification and the utilization of emerging
70 technologies to increase crop yield or protect crop loss have been less utilized (Hazell and Wood
71 2008). In recent years, however, stakeholders, in both the public and private sectors, have sought
72 more innovative approaches - including the use of AI and big data - to protect and improve crop
73 yield. Artificial Intelligence (AI) functions: spatial planning, soil and weather analysis, plant
74 disease and pest detection, precision application of herbicides and pesticides, seasonal forecasting,
75 etc., have the potential to increase agricultural productivity across the continent. A number of these
76 measures are already in use on the continent. Agricultural insurance, used to protect farmers from

77 risks posed by extreme weather phenomena, is another tool that has gained increased usage across
78 the globe.

79 The ability to predict climatic changes using climate models is a critical tool that can be used to
80 develop countermeasures to reduce crop loss, decrease adverse effects on animal husbandry and
81 fishing, and even help insurance companies determine risk for agricultural insurance policies. In
82 this paper, we investigate the efficacy of various open-source climate change models and weather
83 datasets in predicting drought and flood weather patterns in northern and western Kenya. In
84 Section 1, we give a brief overview of climate change models for drought and flood prediction and
85 the weather phenomena experienced in the regions studied; Section 2 and 3 outline the
86 methodology and results of the study; in Section 4, we discuss how the model(s) and dataset(s)
87 determined in Section 3 may be deployed in risk assessment for agricultural insurance, and finally
88 in Section 5, we detail conclusions of the study.

89 1.1. Extreme Weather in Kenya.

90 Kenya's reliance on agriculture and other rain-fed activities to sustain its economy makes it
91 particularly vulnerable to climate extremes. For example, recurring floods in areas along rivers
92 flowing from Lake Victoria: Budalang'i in Busia County, Kano Plains in Kisumu County, and the
93 lower parts of the Tana River area, have led to humanitarian and fiscal disasters (Opere 2013). The
94 variability of extreme rainfall in the country has led to socio-economic challenges in urban and
95 rural settings, including damage to infrastructure, loss of agricultural yields, and adverse effects
96 on human health, e.g., the prevalence of water-related diseases (Juma, et al. 2020). Kenya has also
97 experienced a notable increase in severe and frequent drought events in recent decades. Drought
98 events are predominantly experienced in the eastern and north-eastern regions of the country, as
99 well as parts of the coast and Rift Valley - arid and semi-arid lands (ASAL) that form about 80%
100 of Kenya's land cover (Mutsotso, Sichangi and Makokha 2018, Owuor 2015). The occurrence of
101 drought events in these regions has been exacerbated by the continuous decline in March-May
102 (MAM) seasonal rainfall (Ayugi, Tan and Niu, et al. 2020b). The communities in these areas,
103 mainly pastoralists and agro-pastoralists, are made vulnerable by the adverse effects of the
104 droughts, which include acute malnutrition, famine, increased conflict, interrupted food chains,
105 and economic losses due to poor meat and milk production (Owuor 2015)

106 Research shows that over the past decade, developing countries, on the whole, have incurred over
107 35 billion USD a year in damages from natural disasters, 20 times the cost sustained in the
108 developed world (Mirza 2003). There is growing concern regarding the increase in frequency and
109 magnitude of these extreme weather events. These losses are expected to increase with time. These
110 projections call for continuous assessment and monitoring of the evolving extreme weather
111 patterns in the country, to develop effective adaptation measures to reduce risk and ensure that the
112 region is prepared when unforeseen weather events occur (Kundzewicz, et al. 2014).

113 1.2. Climate Change Modelling for Drought and Flooding Weather Patterns

114 Predicting floods and droughts is important in developing mitigation strategies to manage their
115 impact. The planning of emergency responses and early warning systems rely on flood and drought
116 forecasts at hourly to seasonal time scales (Mizra and Ahmed 2010). Climate change models
117 simulate the future impact of greenhouse gases based on the current understanding of atmospheric

118 physics and chemistry (Hannah 2015). Climate modelling of floods and droughts are typically
119 done separately, primarily because the two types of weather extremes evolve from different
120 processes. Floods are fast phenomena triggered by excess precipitation, snowmelt, high initial soil
121 moisture, or a combination of these factors, while droughts occur slowly triggered by a
122 precipitation deficit and modulated by positive temperature anomalies (Berghuijs, et al. 2016,
123 Brunner, et al. 2021, Hanel, et al. 2018, Wasko and Nathan 2019, Woodhouse, et al. 2016). Two
124 techniques are commonly employed to predict flood and drought weather patterns: driving a
125 hydrological model with meteorological data from a global/regional circulation model (GCM or
126 RCM) or employing hybrid statistical-dynamical techniques using projections as covariates within
127 a statistical modeling framework (Addor, et al. 2014, Hakala, et al. 2019, Madadgar, et al. 2016,
128 Mendoza, et al. 2015, Mizukami, et al. 2016, Slater and Villarini 2018, Wilby 2010).

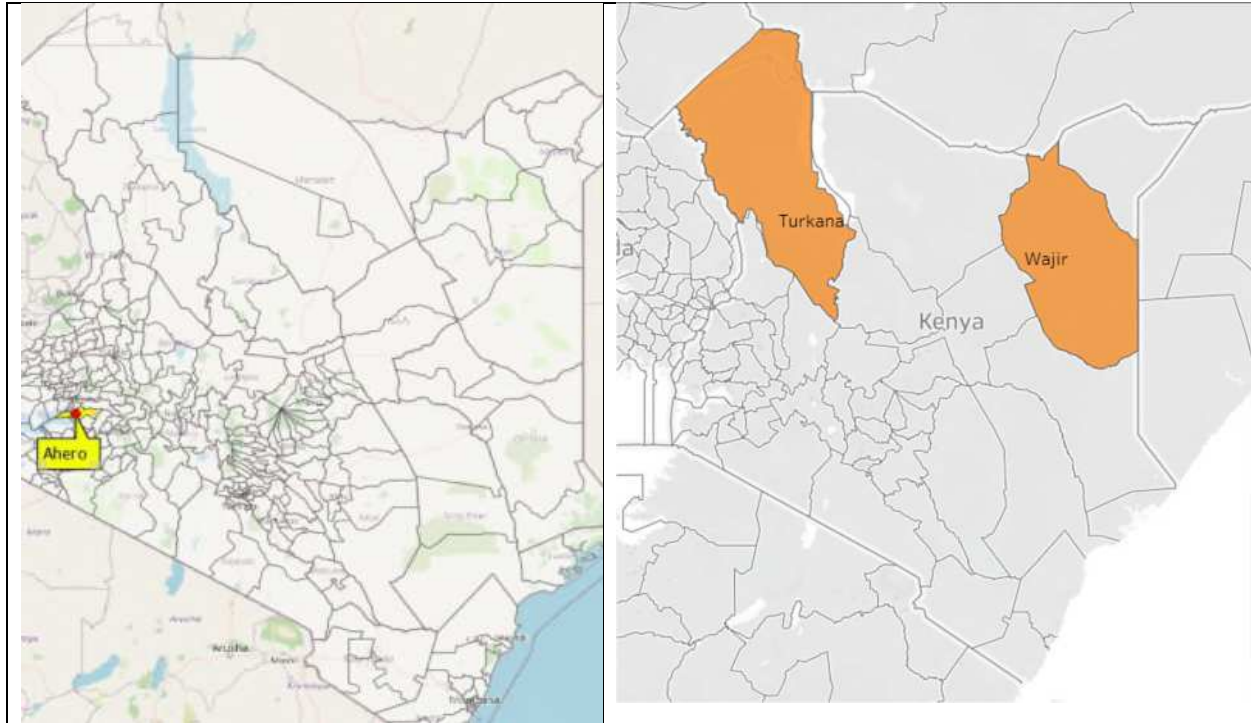
129 Unfortunately, GCMs often have coarse space resolution and cannot represent the fine-scale detail
130 that characterizes the climate in many regions of the world; RCMs, meanwhile, are plagued with
131 uncertainties from boundary conditions, the size of the integration domain, and natural variability
132 within the RCMs and RCM formulation (Luhunga, Botai and Kahimba 2016, Meier, et al. 2011,
133 Min, et al. 2013). In recent years, anomaly detection methods (techniques for identifying
134 unexpected events or patterns that differ from the norm in a given set) have been employed to
135 identify extreme climate events and climate change including floods (Çelik, Dadaser-Çelik and
136 Dokuz 2011, Chalapathy and Chawla 2019, Wibisono, et al. 2021). Density-Based Spatial
137 Clustering of Applications with Noise (DBSCAN) algorithm, nearest neighbourhood-based
138 techniques, and deep learning methods are examples of anomaly detection methods utilized for
139 this purpose. DBSCAN and other clustering-based algorithms identify anomalies as data instances
140 that do not belong to any cluster. Climate modeling studies utilizing the DBSCAN algorithm have
141 shown that this approach is superior to traditional statistical modeling approaches - that the
142 algorithm can identify both extreme and rare anomalies, and it can handle more complex data
143 handling needed for multivariate outlier detection (Çelik, Dadaser-Çelik and Dokuz 2011,
144 Wibisono, et al. 2021). It should be noted that if anomalies were to form clusters, due to the
145 inherent nature of the DBSCAN algorithm, it would be unable to detect them (Chandola, Banerjee
146 and Kumar 2009). Nearest neighborhood-based techniques identify anomalies as instances that
147 occur furthest from their closest neighbors. Studies have shown that the temporal and spatial
148 analysis of anomalies using a k^{th} nearest neighbour (KNN) technique in global climate data could
149 also explain extreme events like drought and flood events at specific locations on earth (Das and
150 Parthasarathy 2009). Compared to clustering-based techniques, nearest neighbourhood-based
151 techniques are better optimised to find anomalies since each instance is evaluated with respect to
152 its local neighbourhood rather than cluster membership (Chandola, Banerjee and Kumar 2009).
153 Finally, deep learning techniques have been used to study anomalies in rich climate data, and are
154 in fact, more adept than traditional statistical methods in dealing with the complex data structures
155 (as they can identify obscure and complex correlations in data sets for which more traditional
156 analysis methods have not determined the underlying model) that characterise climate data, large
157 data volumes and automate feature learning for anomaly prediction (Chalapathy and Chawla
158 2019).

159 Statistical methods have traditionally been used for drought forecasting. Regression, time series
160 analysis, and probability models dominated early attempts in drought forecasting. However, these
161 linear approaches fail to adequately capture the white noise, non-stationary and non-linearity in
162 the time series and thus are gradually being replaced by Artificial Intelligence (AI) models (Fung,
163 et al. 2020). Artificial Neural Networks (ANNs) stand out among the AI models as versatile and
164 well-established drought forecasting tools (Inoubli, et al. 2020). ANNs are flexible, non-linear
165 mathematical modelling systems composed of inter-connected neuron units that mimic the
166 biological nerve system, designed with efficient parallel processing. ANNs learn from the
167 relationships between input parameters and controlled or uncontrolled variables by checking
168 previous trends in historical data as nonlinear regression; the main factors affecting ANNs
169 performance are input adequacy, network architecture and model validation (Deo and Sahin 2015,
170 Fung, et al. 2020).

171 2. Methods

172 2.1. Areas of Study

173 The study focused on three regions in Kenya: Ahero town in Kisumu County, for the flood
174 analysis, and Turkana and Wajir, located in Kenya's most arid area, for the drought analysis as
175 summarized in Fig. 1 The image on the left shows Ahero town, the area of focus for the flood
176 detection study and the image on the right shows Turkana and Wajir counties in Northern Kenya,
177 the areas of interest for the drought study. Ahero is located on the banks of River Nyando. It is
178 commonly known for having low mean rainfall, approximately 7.72mm. However, sporadic high
179 torrential rainfall sometimes leads to pluvial floods in the area. Ahero is among the wards identified
180 in Kenya with high exposure and vulnerability to flooding hazards (Makena, et al. 2021). Turkana
181 is located in the Northern region of Kenya. It has high-temperature levels that range between 36°C
182 and 38°C. Wajir is located in the North-Eastern part of Kenya, where rainfall is scarce and there
183 is low vegetation cover. According to the country's National Drought Management Authority, both
184 of these areas are prone to recurrent drought events (National Drought Management Authority
185 2020, National Management Authority 2020)



186 **Fig. 1** The image on the left shows Ahero town, the area of focus for the flood detection study and
 187 the image on the right shows Turkana and Wajir counties in Northern Kenya, the areas of interest
 188 for the drought study

189 2.2. Datasets

190 Conventionally, three types of datasets are utilized in climate modelling studies: observational
 191 products (satellite or gridded weather station), reanalysis products (obtained by combining
 192 observational inputs and climate models based on physical principles), and simulation products
 193 (climate models). This study used observational and climate datasets (the most commonly used
 194 datasets in data-sparse regions). Monthly precipitation data was obtained for both types of datasets
 195 for the period between 1992-2020.

196 2.2.1. Climate Model Data

197 Climatic data products, generally either GCM or RCM, are used in regions where accessing
 198 accurate and complete meteorological predictors at a high temporal resolution is difficult. At the
 199 regional level, however, GCMs fail to capture complex local processes and land-surface
 200 heterogeneities, which demand spatially detailed information at much finer scales than currently
 201 affordable with GCMs. Regional Climate Models (RCMs) are often used instead. RCMs are
 202 downscaled GCMs to a finer resolution (50km) and consider mesoscale factors such as complex
 203 topography, coastlines, inland bodies of water, and land cover distribution over a limited region of
 204 interest at a computationally affordable cost (Luhunga, Botai and Kahimba 2016, Meier, et al.
 205 2011). Several RCMs of the Coordinated Regional Downscaling Experiment (CORDEX) Africa
 206 have been developed and used for analyses of projections of climatic conditions over East Africa.
 207 Three Regional Circulation Models (RCM) were selected from CORDEX (Coordinated Regional
 208 Downscaling Experiment) for the study:

- 209 • Max Planck Institute for Metrology Germany, MPI-M-MPI-ESM-LR (MPI)
- 210 • Canadian Centre for Climate Modelling and Analysis, CCCma-CanESM2 (CCCma)
- 211 • Met Office Hadley Centre, MOHC-HadGEM2-ES (Had-GEM2)

212 The three RCMs were found in previous studies to reproduce the rainfall climatology over the
213 study domain with reasonable accuracy (Ayugi, Tan and Gnitou, et al. 2020, Luhunga, Botai and
214 Kahimba 2016). The three datasets were applied to the flood detection model, while the drought
215 prediction models used the MPI and Had-GEM2.

216 2.2.2. Satellite Data

217 Two satellite datasets were utilized: CHIRPS (Climate Hazards Group Infrared Precipitation with
218 Station data) and TAMSAT (Tropical Applications of Meteorology using Satellite data and
219 ground-based observations). CHIRPS is a quasi-global rainfall dataset that incorporates a 0.050
220 (4.4km) resolution. It is mostly used in drought and flood monitoring. The University of Reading
221 established TAMSAT to enhance the use of satellite-based rainfall estimates in Africa (Maidment,
222 Black and Young 2017). The satellite uses a 4km resolution in the capturing of the rainfall data.
223 Both satellite datasets have data spanning from 1992 to 2020 and are strictly for rainfall and
224 therefore only utilized by the flood detection model.

225 2.2.3. Weather Station Data

226 Weather station data provides inferences for a single point compared to satellite or climate model
227 datasets which capture a much larger area (TAMSAT and CHIRPS 4km resolution and RCMs
228 50km resolution). Weather station data was obtained from the Visual Crossing Weather Platform
229 (<https://www.visualcrossing.com>), which provides daily historical forecasted data from any
230 geographic location. The platform builds its historical weather data by combining raw surface
231 observational data from various meteorological observational datasets such as the Integrated
232 Surface Database (ISD) and the Meteorological Assimilation Data Ingest System (MADIS). The
233 data acquired for this study spans the period from 1992 to 2020. Two additional datasets were also
234 used: Trans-African Hydro-Meteorological Observatory (TAHMO), which was used to confirm
235 the data bias of the visual crossing data, and World Weather Online data, which provides intra-day
236 periods of data (3-hour data up to 1-hour data) for finer forecasts of the data. Weather station data
237 have both temperature and rainfall data and are therefore applicable to the drought and flood
238 models.

239 2.3. Anomaly Detection Techniques and Performance Evaluation for Flood Detection

240 Four unsupervised anomaly detection techniques were utilized in the flood study: K-Nearest
241 Neighbours (KNN), Histogram-Based Outlier Score (HBOS), Cluster-Based Outlier Factor
242 (CBLOF), and Isolation Forests.

243 K-Nearest Neighbours (KNN) is one of the simplest anomaly detection methods. It is a supervised
244 machine learning algorithm that takes an unsupervised approach to anomaly detection. This
245 density-based measure assumes that normal data points occur around a dense neighbourhood and
246 anomalies lie far away. The algorithm performs a nearest neighbour search by computing distances
247 of every two data points then compares them to an arbitrary threshold value beyond which
248 observations are identified as anomalies (Chandola, Banerjee and Kumar 2009). The main

249 advantage of the KNN technique is that it is straightforward to adapt to different data types and
 250 only requires the definition of K and an appropriate distance measure for the given data. The study
 251 utilised a contamination rate of 10% with a K threshold of 5 and the Minkowski distance measure,
 252 a generalisation of the Euclidean and Manhattan distance measures.

253 Histogram-Based Outlier Score (HBOS) is a statistical-based anomaly detection technique
 254 (Goldstein and Dengel 2012). HBOS assumes that the data set features are independent and models
 255 the feature densities using normalised histograms (maximum height = 1) with a static or dynamic
 256 bin width. The height of every single bin of the histogram represents the density estimation. The
 257 outlier score for every data point is a multiplication of the inverse of the estimated densities,
 258 defined as:

$$259 \quad HBOS(x) = \sum_{i=0}^d \log\left(\frac{1}{hist_i(x)}\right)$$

260 *Equation 1: Density Estimation represented by a single bin in Histogram Based Outlier Score (HBOS) calculation*

261 where: d represents the number of features in the data set, $hist_i(v)$ is the density estimation of
 262 each feature instance, and x is the vector of features. Higher scores represent anomalies that would
 263 intuitively be assigned to bins with low density. This technique is fast compared to other
 264 techniques. For instance, it has a linear time complexity $\mathcal{O}(n)$ compared to KNN's $\mathcal{O}(n^2)$. HBOS is
 265 also a suitable option for treating global anomalies. However, it is a poor choice for local
 266 anomalies.

267 Cluster-based Local Outlier Factor (CBLOF) is an anomaly detection technique that combines a
 268 nearest neighbour-based technique, Local Outlier Factor (LOF), and clustering for data pre-
 269 processing and anomaly identification (He, Xu and Deng 2003). The algorithm assigns each data
 270 point a CBLOF, which is determined by the distance of the data point to its nearest neighbour and
 271 the size of its cluster. Anomalies are identified as instances that belong to small or sparse clusters.
 272 CBLOF was designed to address shortcomings in clustering-based methods such as DBSCAN and
 273 nearest neighbour-based approaches such as Local Outlier Factor that were deemed ineffective.
 274 The technique is better at capturing local anomalies than HBOS. Additionally, its computational
 275 cost is minimised by distributing large data sets into meaningful clusters. To calculate the CBLOF,
 276 k-means is used to cluster the dataset. Then a heuristic procedure is applied to split the clusters
 277 into two categories based on their density. The anomaly score is defined as:

$$278 \quad CBLOF(x) = \begin{cases} |C_i|^* \min(\text{distance}(x, C_j)), & \text{if } x \in C_i, C_i \in SC \text{ and } C_j \in LC \text{ for } j = 1 \text{ to } b \\ |C_i|^* \min(\text{distance}(x, C_i)), & \text{if } x \in C_i \text{ and } C_i \in LC \end{cases}$$

279 *Equation 2: Anomaly score in Cluster-based Local Outlier Factor (CBLOF) calculations.*

280 where: C_i and C_j represent clusters, $LC = C_i \mid i \leq b$ represents large clusters, $SC = C_j \mid j > b$
 281 represents small clusters, and b is the cluster boundary (small or large).

282 Isolation Forests is an anomaly detection method for continuous data (Liu, Ting and Zhou 2012).
 283 The isolation forests technique makes two assumptions about anomaly data: anomalies vary

284 significantly from normal observations making it easy to isolate, and anomaly data are rare in the
 285 dataset. Given these assumptions, isolation of anomalies is implemented using an isolation tree
 286 (*iTree*), which is a binary tree structure that considers whether an observation is an anomaly or
 287 not. The algorithm recursively portions a dataset to build an ensemble of *iTrees*. The anomaly
 288 score is derived from the path length, averaged over the isolation trees' ensemble. Anomalies are
 289 identified as instances with short average path lengths on the *iTrees*. Isolation Forests have several
 290 advantages over other anomaly detection techniques. First, given its base assumptions, the
 291 algorithm can exploit subsampling, making it fast and scalable. Second, Isolation Forests can
 292 detect both clustered and scattered anomalies in the global context of the entire dataset. Isolation
 293 Forests requires two training parameters: the number of trees to build and sub-sampling size and
 294 one evaluation parameter: the tree height limit during evaluation. The anomaly score for every
 295 data point x is defined as:

$$296 \quad s(x, n) = 2 \frac{E(h(x))}{c(n)}$$

297 *Equation 3: Anomaly score for individual data points in the Isolation Forest calculation.*

298 where: $E(h(x)) = \frac{\sum_{i=1}^t h_i(x)}{t}$ is the average path length of x over t *iTrees*, $c(n) = 2H(n - 1) -$
 299 $\left(\frac{2^{(n-1)}}{n}\right)$ with $H(i) = \ln(i) + \gamma$ (γ is Euler's constant), the average path length of unsuccessful
 300 search in Binary Search Tree (BST). If $s(x, n)$ of x is close to 1, x is considered an anomaly or if
 301 less than 0.5, x is considered normal. The isolation forest contamination rate for the study was set
 302 to 10% such that the confidence interval was at 90% for the flood detection rate to ensure high
 303 precision for anomaly identification.

304 Model performance was done by comparing model data with the Standardised Precipitation Index
 305 (SPI). SPI quantifies precipitation anomalies for long-term normal conditions on multiple time
 306 scales (McKee, Doesken and Kleist 1993). Computation of the SPI involves fitting a probability
 307 distribution to an aggregated monthly precipitation time scale that may range from 3-48 months.
 308 The probability function is then transformed into a normal standardised index that is traditionally
 309 classified into flood classes that characterise the flood severity at each place and time scale. This
 310 study computed the SPI by fitting a logistic distribution for the different precipitation time series
 311 data. The data was converted to monthly intervals to maintain low granularity. SPI values greater
 312 than two were treated as the true observations of the occurrence of a flood. Using the SPI values
 313 to label the occurrence of flood events, the study measured how well the anomaly detection models
 314 predicted the actual class of the data point using the following metrics:

- 315 • Fraction Accuracy, which measured the fraction of the flood occurrences discovered by the
 316 outlier detection models over the number of floods the SPI found.
- 317 • Specificity, which measured how well the model was able to determine when floods would
 318 not occur.

$$319 \quad \frac{TN}{TN + FP}$$

- 320 • Sensitivity, which measured how well the model detected flood occurrences.

321
322
323
324
325
326
327
328
329
330
331
332
333
334
335
336
337
338
339
340
341
342
343
344
345
346
347
348
349
350
351
352
353
354
355
356
357

$$\frac{TP}{TP + FN}$$

Note: TP is defined as the true positives from the model, TN is the model's true negatives, FP the false positives and FN the false negatives from the model.

- AUC-ROC, which measured the ability of the anomaly detection methods to distinguish between flood and normal observations.

2.4. ANN Model Development and Performance Evaluation for Drought Prediction

The ANNs were developed using the output from the Standardised Precipitation Evapotranspiration Index (SPEI) values for 28 years (1992-2020). SPEI is computed using precipitation and the potential evapotranspiration (PET) data to define anomalous wet and dry conditions by normalising the monthly (or weekly) difference between water supply (precipitation) and demand (potential evapotranspiration). This study calculated the PET following the Hargreaves equation (Hargreaves and Samani 1985). The Hargreaves equation uses the daily difference between the maximum and minimum as a proxy to estimate net radiation and simplifies the mass transfer term with a constant. Additionally, the study found the Hargreaves equation to be more suited to monthly durations.

$$PET = 0.0023 \times R_A \times TD^{0.5}(TC^\circ + 17.8)$$

where: R_A measures the extra-terrestrial radiation calculated by knowing the station latitude, TD is the mean maximum minus the mean minimum temperature, TC is the mean temperature in degrees Celsius. The accumulated water profit or loss series, D_n^k , is computed using the following formula:

$$D_n^k = \sum_{i=0}^{k-1} P_{n-i} - PET_{n-i}, \quad n \geq k$$

where: P_i is the monthly precipitation, PET_i is the monthly potential evapotranspiration, k is the time scale in months, and n is the calculation frequency. The D series was standardised using the log-logistic distribution based on the behaviour of the extreme values (Vicente-Serrano, Beguería and López-Moreno 2010). A log transformation was performed to normalise the input values and control for extreme values in the data. The study converted the SPEI time series into binary data indicating whether a given period experienced drought or normal conditions.

We utilized a multi-layer perceptron (MLP), neural network model, along with a user-created neural network. The selected ANNs used a two-layer neural network with four input layers, eight hidden layers and one output layer. The models used feed-forward backpropagation (BPN) as the training algorithm. The BPN utilised a sigmoid activation function since the output is of a binary form. A learning rate of 0.0001 was used to maximise the creation of the best log loss slope – for all the models, the same parameters were put in place to see how they all differ.

The data was split into a train-test and validation set up for each data set, where 90% of the data was used for training and testing (80:20). The remaining 10% was used in the validation. The training data consisted of the minimum and maximum temperature and precipitation variables. The

358 SPEI value grading for drought analysis was capped at < -1.5 to signal the start of drought
 359 occurrences.

360 The performance of the ANN models in predicting the monthly SPEI was statistically evaluated
 361 using the accuracy score and the AUC-ROC.

- 362 • The accuracy score measures the fraction of correct predictions out of the total number of
 363 observations.

$$364 \quad Accuracy = \frac{TP + TN}{TP + FP + FN + TN}$$

- 365 • The AUC-ROC measures the models' capacity to distinguish between drought and normal
 366 observations.

367 3. Results

368 3.1. Flood Detection in Ahero County in Western Kenya

369 Four anomaly detection models (CBLOF, HBOD, KNN, IF) and six datasets (CHIRPS, MPI, Had-
 370 GEM2, TAMSAT, CCCma, Weather Station Data) were analysed to determine their accuracy in
 371 detecting floods in Ahero county. Table 1 summarises descriptive statistics of precipitation data
 372 obtained from the selected open-source observational and simulation datasets. The datasets varied
 373 greatly in terms of precipitation distribution. TAMSAT data recorded the highest mean
 374 precipitation of 3.84mm (± 0.79), while the weather station data had the highest maximum
 375 precipitation recorded over the study period, 236mm. The RCMs recorded the lowest precipitation
 376 over the period compared to the observational products. The Met Office Hadley Centre Regional
 377 Climate Model (Had-GEM2) had the lowest average rainfall of 0.57 mm (± 2.43). The differences
 378 between observed and simulated annual rainfall have been attributed to the poor skill of RCMs in
 379 reproducing the regional climate over East Africa (Ayugi, Tan and Gnitou, et al. 2020, Bichet, et
 380 al. 2020, Mumo and Yu 2020).

381 Table 1: A comparison of precipitation data for Ahero county across the 6 different datasets
 382 analyzed.

	MPI	CCCMA	HAD- GEM2	CHIRPS	TAMSAT	WEATHER STATION
NUMBER OF DAYS	10,593	10,593	10,593	10,593	10,593	10,573
MEAN PRECIPITATION	0.95	0.65	0.57	0.79	3.84	1.13
SD PRECIPITATION	3.48	2.7	2.43	4.10	4.79	8.44
MIN PRECIPITATION	0.00	0.00	0.00	0.00	0.00	0.00

**MAX
PRECIPITATION**

48

34

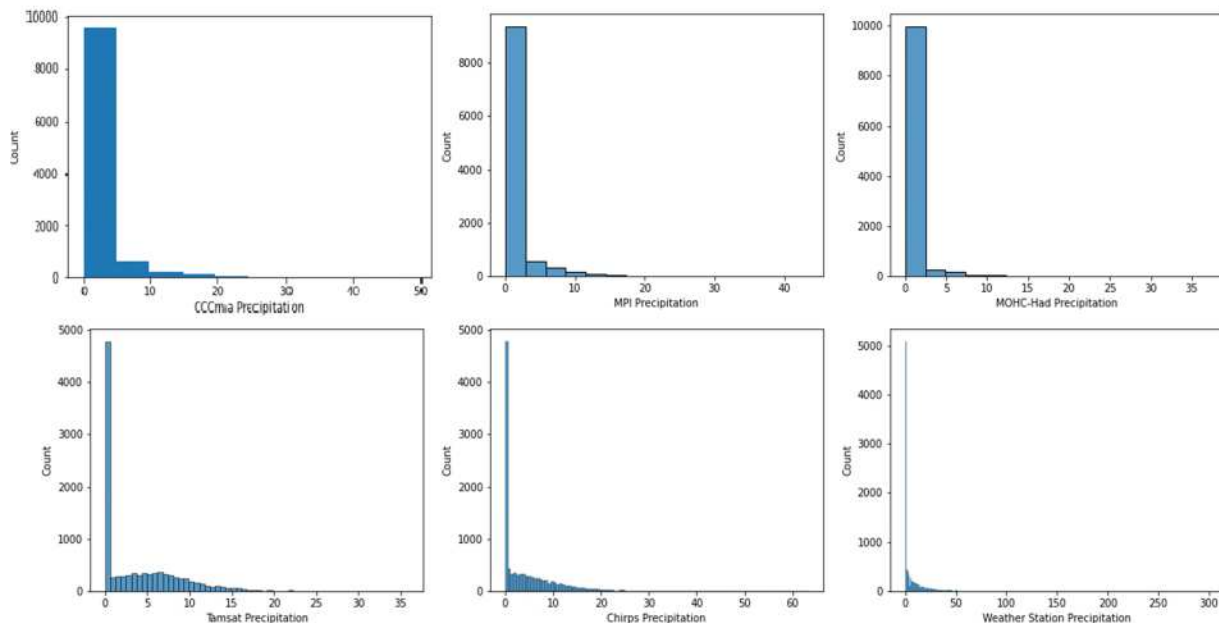
35

70.07

35.90

236.00

383 Fig. 2 illustrates the precipitation distribution in Ahero over the observation period and highlights
384 the differences in precipitation data across the datasets. Precipitation over the region features a
385 positive skew, with few instances of extreme rainfall. This distribution is carried across all datasets.
386 However, we find that the precipitation data obtained from RCMs recorded no or low precipitation
387 in the region over the observation period compared to the other datasets. Previous evaluations of
388 RCM performance over the East African region found RCMs underestimate rainfall, especially
389 during the March-April-May (MAM) seasons (Luhunga, Botai and Kahimba 2016). Previous
390 studies report the poor performance of RCMs of the region in reproducing rainfall events when
391 compared to observational data is attributed to various factors, including their different abilities to
392 simulate mechanisms behind rainfall formation over the region due to the paucity of in situ data
393 required for model parameterization (Mumo and Yu 2020).



394

395 *Fig. 2 Distribution of precipitation across the selected datasets: CCCma, MPI, Had-GEM2 TAMSAT, CHIRPS, and Weather*
396 *Station Data*

397 The number of floods identified by the SPI varied with each dataset. The variation in the number
398 of floods across the selected datasets is due to the differing mechanisms in which the data products
399 estimate rainfall. Each model performance was assessed against the unique characteristics of the
400 data used; model performance varied with each dataset. In general, the anomaly detection models
401 were able to identify more than half of the flood anomalies in the CHIRPS dataset but performed
402 poorly in identifying flood anomalies in the climate model datasets. The best performance was
403 obtained by the CBLOF anomaly detection method using the CHIRPS dataset. 80% of the
404 anomalies detected had been identified as flood events based on the SPI. Precipitation distribution
405 in the RCM datasets may be the reason for their poor performance in flood detection; most of the
406 observations in the RCM data had no or low precipitation values recorded. Table 2 details the

407 number of flood anomalies detected by each model as a fraction of the number of floods identified
 408 by the SPI (last row):

409 Table 2: Algorithm performance calculated as a function of the number of floods detected
 410 compared to the number identified by SPI.

	CHIRPS	WEATHER STATION	TAMSAT	CCCMA	MPI	HAD- GEM2
CBLOF	80%	34%	25%	5%	1%	0%
HBOD	67%	46%	-	5%	1%	0%
IF	67%	33%	20%	1%	1%	0%
KNN	67%	40%	50%	5%	1%	-
No. Floods SPI	30	19	17	28	23	24

411 Model specificity was determined for each type of dataset. All models performed well in terms of
 412 classifying non-flood events correctly when using weather station data but were less accurate when
 413 utilizing climate model data. Table 3 summarizes the model specificity:

414 Table 3: Model specificity in classifying non-flood events

	WEATHER STATION	CHIRPS	TAMSAT	CCCMA	HAD-GEM2	MPI
HBOD	1	0.17	0	0	0	0
CBLOF	1	0.14	0	0	0	0
IF	1	0.17	0	0	0	0
KNN	1	0.25	0	0	0	0

415

416 Additionally, model sensitivity was determined against each type of dataset. All four models were
 417 able to identify flood anomalies correctly for each of the six dataset types (Table 4). However, this
 418 may be attributed to the zero-inflation (distribution that allows for frequent zero-valued
 419 observations) of the TAMSAT and the climate model data, indicating how skewed these datasets
 420 are in the detection of floods.

421

422 Table 4: Model sensitivity that measures the model ability to identify flood anomalies.

	WEATHER					
	CHIRPS	STATION	TAMSAT	CCCMA	HAD-GEM2	MPI
HBOD	0.97	1	1	1	1	1
CBLOF	0.96	1	1	1	1	1
IF	0.97	1	1	1	1	1
KNN	0.944	0	1	1	1	1

423 Finally, Table 5 summarizes the area under the curve receiver operating characteristic (AUC-ROC)
 424 performance measure, which provides information on the models' ability to differentiate between
 425 flood and non-flood events. Isolation Forests model using weather station data had the best
 426 performance in distinguishing between flood events with an AUC-ROC measure of 0.8. Unlike
 427 HBOD, CBLOF and KNN, IF models identify anomalies independent of the underlying data
 428 distribution; the other anomaly detection algorithms build a profile of normal instances based on
 429 distance or density; high-density regions or short distances measured in a local context could be
 430 anomalies in the global data set or vice versa. Isolation forest path-length-based isolation traverse
 431 data to identify anomalies in local and global contexts. This may account for the discrepancies in
 432 performance between the 4 models. The CBLOF model also had good performance with the same
 433 dataset. The models performed especially poorly using data from the regional climate models. All
 434 models could not differentiate between flood and non-flood events using RCM data. The poor
 435 performance may be attributed to the precipitation distribution, which underestimated rainfall in
 436 the region, leading to an inflation of zeros in the dataset.

437 Table 5: Algorithm performance in differentiating between flood and non-flood events as
 438 ascertained using the AUC- ROC performance measure.

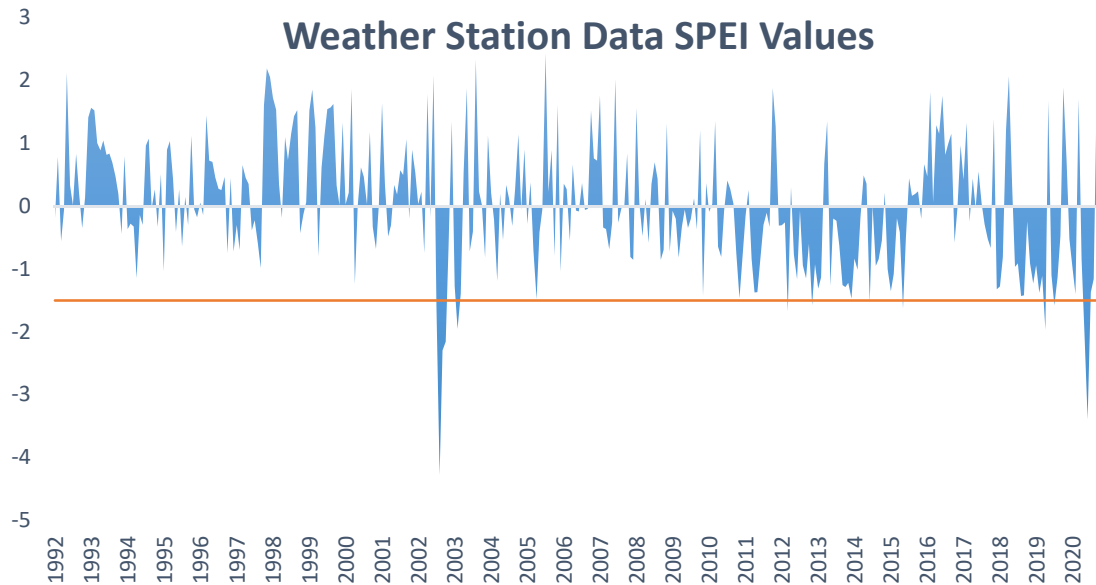
	WEATHER					
	CHIRPS	STATION	TAMSAT	CCCMA	HAD-GEM2	MPI
HBOD	0.57	0.5	0.5	0.5	0.5	0.5
CBLOF	0.55	0.732	0.5	0.5	0.5	0.5
IF	0.566	0.8	0.5	0.5	0.5	0.5
KNN	0.597	0.5	0.5	0.5	0.5	0.5

439 3.2. Drought Detection in Turkana and Wajir Counties in Northern Kenya

440 3.2.1. Drought Detection using SPEI

441 SPEI was computed for the selected region using the three datasets. Fig. 3, Fig. 4, Fig. 5 summarize
 442 the 1-month SPEI variability in the three datasets for the period between 1992-2020 in Turkana
 443 and Wajir counties. Positive SPEI values indicate greater than normal precipitation, while negative
 444 values indicate less than normal precipitation. Therefore, extreme peaks and troughs in the graphs
 445 indicate flood or drought events, respectively. A cutoff point of -1.5 was used to identify extreme
 446 drought events in the two regions in the study. There is evidence of within-season variability with

447 experiences of moderate to severe and moderate to extreme drought cases within the period.
448 Examining Fig. 3, 1-month SPEI values computed from weather station data shows dry events in
449 the region occur towards the end of 2002 and early 2003; another long dry event starts in 2012 and
450 ends in 2015 with intermittent wet periods, and again in the period from 2019-2020. Extreme
451 drought events occurred in 2012 and the start of 2020.

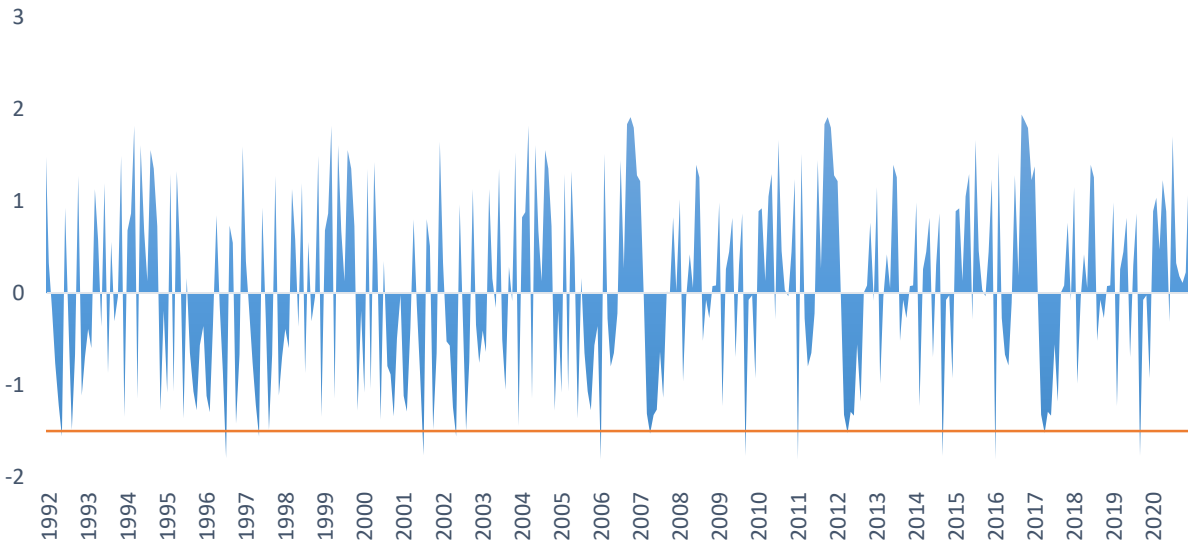


452

453 *Fig. 3 1-month SPEI variability in Weather Station Data for the years 1992-2020*

454 The MPI and Had-GEM2 RCMs capture several instances of drought events as summarized in Fig.
455 4 and Fig. 5 respectively. Moderate drought events were observed during the period 1992, 1996,
456 1997, 2001, 2002, 2007, 2009, 2011, 2012, 2014, 2016, 2017 and 2019 for MPI. While the Had-
457 GEM2 captured extreme drought events in 2001, 2010, 2015 and 2020 in addition to the moderate
458 events captured by the MPI dataset.

MPI RCM 1-Month SPEI Values

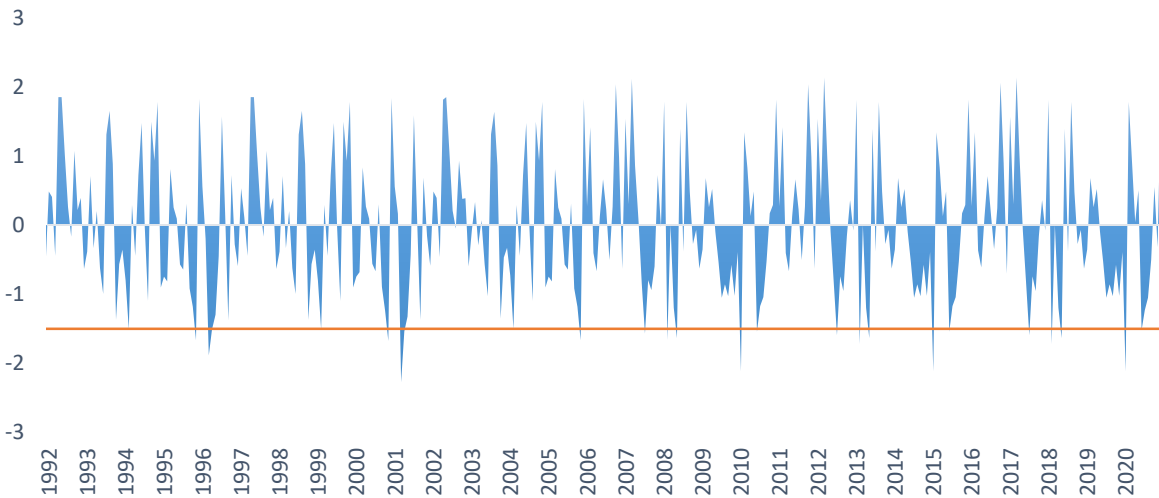


459

460

Fig. 4 1-month SPEI variability in MPI RCM for the years 1992-2020

HAD-GEM2 RCM 1-Month SPEI Values



461

462

Fig. 5 1-month SPEI variability in Had-GEM2 RCM for the years 1992-2020

463

464

465

466

467

The droughts captured in the observational data and the regional climate models correspond to drought incidences reported in the literature (Ayugi, Tan and Gnitou, et al. 2020, Ayugi, Tan and Niu, et al. 2020b, Owuor 2015). However, the time and frequency of drought instances differed between the datasets. The discrepancies can again be attributed to varying precipitation distribution between the observed weather station data and simulated RCM datasets.

468 3.2.2. ANN Drought Forecasting Model
 469 Different ANNs were tested for forecasting the SPEI using weather station data and climatic model
 470 data. Table 6 lists the accuracy scores for the training and validation period. There is some
 471 reduction in the evaluation metric during the validation period. The low values in the validation
 472 period indicate that there is possibly some zero inflation, where the model predicts one scenario
 473 overall. Weather station data using the MLP neural network gave the best performance for 1-month
 474 drought forecasting. It had the highest training and validation accuracy scores and the lowest
 475 reduction in accuracy scores between training and validation. Among the regional climate models,
 476 Met Office Hadley Centre, MOHC-HadGEM2-ES (Had-GEM2) provided the best validation
 477 accuracy at 57%.

478 Table 6: Accuracy Scores of ANNs for 1-month Drought Forecasting of SPEI

	WEATHER STATION DATA		MPI		HAD-GEM2	
	Training	Validation	Training	Validation	Training	Validation
USER-CREATED NEURAL NETWORK	90%	48%	87%	45%	81%	57%
MULTI-LAYER PERCEPTRON (MLP) NEURAL NETWORK	78%	63%	63%	54%	70%	57%
VALIDATION ACCURACY	73%		63%		40.8%	

479
 480 ANN models using weather station data had the highest AUC-ROC scores - indicating that the
 481 developed models could adequately distinguish between drought and non-drought events (Table
 482 7). The regional climate models had low scores in this respect except for the MOHC-HAD data
 483 using the MLP neural network. Additionally, AUC-ROC increased to 0.65 in the validation period
 484 for weather station data, indicating the model's generalisability. The regional climate models, MPI
 485 and MOHC-HAD, had much lower scores in this respect, with the exception of the MOHC-HAD
 486 data using the MLP neural network. MLP performance was superior to the user-generated neural
 487 network due to the use of an Adam optimiser. The discrepancies between the RCM and Weather
 488 Station data results are difficult to attribute to a specific source. RCMs have deficiencies in
 489 projecting the observable climate in the East African region, but weather station data accuracy is
 490 also limited (generally, by the number of weather stations used for interpolation, incompleteness,
 491 or inaccuracies of station records).

492 Table 7: AUC-ROC Scores for the ANNs

	WEATHER STATION DATA	MPI	HAD-GEM2

MULTI-LAYER PERCEPTRON NEURAL NETWORK (MLP)	0.6	0.45	0.62
--	-----	------	------

493 It is worth noting that model and dataset performance could only be evaluated against SPEI values
 494 as there are no drought or flood repositories with historical weather data on these phenomena in
 495 Kenya. Ground truth data is needed to validate the above findings.

496 4. Discussion and Conclusion

497 The main resource for agricultural production, the land, is heavily affected by agro-climatic
 498 conditions - meteorological events heavily influence crop farming and animal husbandry
 499 outcomes. Thus, extreme weather events often adversely impact farmers and pastoralists; and
 500 contribute to rural poverty. Farmers can lose their crops, means of production, and even access to
 501 their land through extreme weather events like floods and droughts. An increase in the intensity
 502 and frequency of these extreme weather events due to climate change will result in a corresponding
 503 increase in the negative impacts on agricultural productivity. Agricultural insurance, provided by
 504 government or private entities, can be a risk mitigation tool for farmers.

505 Agricultural insurance reduces the risks of lending to the farming sector by enabling farmers and
 506 pastoralists a means of repaying loans; eases budget volatility of agriculture-related fiscal
 507 expenditures by transferring climatic risk to the private sector; increases fiscal stability during
 508 crisis events and stimulates growth of the agricultural sector (Baskaran and Maher 2021). In
 509 Kenya, for example, as part of the response to the 2008 – 2011 drought, the government
 510 implemented a National Disaster Risk Financing Strategy, under which an agriculture insurance
 511 program, implemented in partnership with the private sector, targets vulnerable farmers; as of early
 512 2021, more than half a million farmers were insured against agricultural losses under the program
 513 (Baskaran and Maher 2021). For the process to work successfully, however, insurance companies
 514 must have access to high-quality data to determine the risks of insuring farmers, agro-pastoralists,
 515 pastoralists, and their small businesses – a process known as underwriting. Underwriting, in
 516 addition to determining the risks posed by a prospective policyholder, also determines the cost of
 517 coverage. We contend that climate change models, with their ability to predict drought or flooding
 518 conditions, could be an indispensable part of the underwriting process.

519 Traditionally, calculation of risk for agricultural insurance involved analysis of yield data.
 520 However, this process is often undermined by the lack of high-quality yield data especially in rural
 521 regions, like the three regions in this study. An alternative to yield data is employing index-based
 522 insurance (IBI), e.g., rainfall-based index insurance. Index-based insurance relies on the measured
 523 value of an objective and independent index; the payment to the insured is based not on the
 524 assessment of the insured's actual loss but on the measured value from the index, i.e., the index
 525 serves as a proxy for the actual loss (Kenya Insurance Regulatory Authority 2015). For example,
 526 indemnity payments for the Kilimo Salama insurance in Kenya, Tanzania and Rwanda, and the
 527 Nyala Insurance Share Company (NISCO) in Ethiopia, are made for the insured crop, when actual
 528 rainfall in the cropping season, recorded in the nearest weather station, falls below predefined
 529 threshold levels (Dercon, et al. 2014, Wairimu, Obare and Odendo 2016). IBI can reduce the costs
 530 and difficulties of administering and delivering agricultural insurance. Index-based insurance

531 would necessitate the development of a model that related weather phenomena such as floods or
532 drought, linearly or non-linearly, to risk. An important step in this process would be accurately
533 determining the occurrence, and intensity, of future drought and flood events.

534 In this study, we identified two models that may be used to predict flood and drought events. The
535 combination of ANNs and weather station data was the most effective in predicting future drought
536 occurrences in Turkana and Wajir counties (both drought-prone regions) with accuracies ranging
537 from 78% to 90%. In the case of flood forecasting, Isolation Forests models using weather station
538 data had the best overall performance. The study also found that the regional climatic models (Max
539 Planck Institute for Metrology Germany, MPI-M-MPI-ESM-LR (MPI; Canadian Centre for
540 Climate Modelling and Analysis, CCCma-CanESM2 (CCCma), and Met Office Hadley Centre,
541 MOHC-HadGEM2-ES (Had-GEM2)) utilized struggled to identify flood anomalies in Ahero
542 county (all three model performance of monthly aggregation was very low) but the RCMs from
543 CORDEX-Africa (Max Planck Institute for Metrology Germany, MPI-M-MPI-ESM-LR (MPI)
544 and Met Office Hadley Centre, MOHC-HadGEM2-ES (MOHC-HAD)) utilised in the study had
545 adequate performance in drought forecasting. Superior weather station data performance, in both
546 flood and drought forecasting, could be attributed to the single-point measurements provided by
547 weather station data which are usually more accurate when compared to reanalysis or simulation
548 data products. This suggests that improvements in coverage of weather station data in data-sparse
549 regions would increase the accuracy in drought and flood forecasting of climate models which
550 would, in turn, increase accuracy in the underwriting process.

551 IBI powered by predictive climate change models could democratize risk information. Since IBI
552 would be based on an independent variable determined by the climate change models, and not the
553 actual crop or animal loss, then the insurance companies could make information on risk and the
554 resultant cost of coverage available to farmers ahead of the farming season for a particular crop.
555 This would give farmers ample time to decide: (i) whether they needed coverage, (ii) what type of
556 coverage they required, and (iii) how they would finance the cost of the policy. Coupling climate
557 change models (with high predictive accuracy) to the IBI underwriting process would reduce basis
558 risk – the risk that what is predicted by the index differs from farmers’ experiences. A reduction
559 in basis risk would increase farmers’ trust in insurance coverage and is likely to increase the
560 number of farmers who elect to obtain agricultural insurance coverage. This would lead to greater
561 economic stability for individual farmers and rural communities (who predominantly rely on
562 agricultural activities for revenue) as a whole. Using climate modelling in the underwriting process
563 will ensure that the risk calculation process is an objective one – reducing ethical issues of human
564 bias in determining coverage and cost of coverage. Finally, flood and drought trends predicted by
565 the climate models may be used by the insurance companies to generate additional mitigation
566 factors in a policy to aid farmers in reducing crop or animal loss from these extreme weather
567 phenomena.

568 We intend, in the second phase of this project, to develop a model that utilizes the two identified
569 drought and flood predictive climate change models, ANN and Isolated Forest models with
570 weather station data, respectively, to calculate risks of crops grown in the regions of the study

571 mentioned in this paper. This model will be analysed against current methods of calculating risk
572 for agricultural insurance policies in Kenya to determine which process is more efficacious.
573
574

575 References

- 576 Addor, N., O. Rössler, N. Köplin, M. Huss, R. Weingartner, and J. Seibert. 2014. "Robust changes
577 and sources of uncertainty in the projected hydrological regimes of Swiss catchments."
578 *Water Resources Research* 50 (10): 7541 - 7562.
579 doi:<https://doi.org/10.1002/2014WR015549>.
- 580 Ayugi, B., G. Tan, G. T. Gnitou, M. Ojara, and V. Ongoma. 2020. "Historical evaluations and
581 simulations of precipitation over East Africa from Rossby centre regional climate model."
582 *Atmospheric Research* 232: 104705. doi:<https://doi.org/10.1016/j.atmosres.2019.104705>.
- 583 Ayugi, B., G. Tan, R. Niu, Z. Dong, M. Ojara, L. Mumo, H. Babaousmail, and V. Ongoma. 2020b.
584 "Evaluation of meteorological drought and flood scenarios over Kenya, East Africa."
585 *Atmosphere* 11 (3): 307. doi:<https://doi.org/10.3390/atmos11030307>.
- 586 Baskaran, G., and B. Maher. 2021. *Agricultural insurance: The antidote to many economic*
587 *illnesses*. Brookings Institute. May 26. Accessed September 20, 2021.
588 [https://www.brookings.edu/blog/future-development/2021/05/26/agricultural-insurance-](https://www.brookings.edu/blog/future-development/2021/05/26/agricultural-insurance-the-antidote-to-many-economic-illnesses/)
589 [the-antidote-to-many-economic-illnesses/](https://www.brookings.edu/blog/future-development/2021/05/26/agricultural-insurance-the-antidote-to-many-economic-illnesses/).
- 590 Berghuijs, W. R., R. A. Woods, C. J. Hutton, and M. Sivapalan. 2016. "Dominant flood generating
591 mechanisms across the United States." *Geophysical Research Letters* 43 (9): 4382-4390.
592 doi:<https://doi.org/10.1002/2016GL068070>.
- 593 Bichet, A., A. Diedhiou, B. Hingray, G. Evin, N. Touré, K. N. A. Browne, and K. Kouadio. 2020.
594 "Assessing uncertainties in the regional projections of precipitation in CORDEX-
595 AFRICA." *Climatic Change* 162 (2): 583-601. doi:[https://doi.org/10.1007/s10584-020-](https://doi.org/10.1007/s10584-020-02833-z)
596 [02833-z](https://doi.org/10.1007/s10584-020-02833-z).
- 597 Bjornlund, V., H. Bjornlund, and A.F. Van Rooyen. 2018. "Why agricultural production in sub-
598 Saharan Africa remains low compared to the rest of the world – a historical perspective."
599 *International Journal of Water Resources Development* 36 (1): 20 - 53.
600 doi:<https://doi.org/10.1080/07900627.2020.1739512>.
- 601 Boko, M., I. Niang, A. Nyong, C. Vogel, A. Githeko, M. Medany, B. Osman-Elasha, R. Tabo, and
602 P. Yanda. 2007. "Africa. Climate Change 2007: Impacts, Adaptation and Vulnerability."
603 In *Contribution of Working Group II to the Fourth Assessment Report of the*
604 *Intergovernmental*, by M.L. Parry, O.F. Canziani, J.P. Palutikof, P.J. van der Linden and
605 C.E. Hanson, 433-467. Cambridge, UK: Cambridge University Press.
606 <https://cgspace.cgiar.org/handle/10568/17019>.
- 607 Brunner, M. I., L. Slater, L. M. Tallaksen, and M. Clark. 2021. "Challenges in modeling and
608 predicting floods and droughts: A review." *Wiley Interdisciplinary Reviews: Water* 8 (3):
609 e1520. doi:<https://doi.org/10.1002/wat2.1520>.
- 610 Çelik, M., F. Dadaser-Çelik, and A. Ş. Dokuz. 2011. "Anomaly detection in temperature data using
611 DBSCAN algorithm." *2011 International Symposium on Innovations in Intelligent Systems*

- 612 *and Applications.* Istanbul: IEEE. 91-95.
613 doi:<https://doi.org/10.1109/INISTA.2011.5946052>.
- 614 Chalapathy, R., and S. Chawla. 2019. "Deep learning for anomaly detection: A survey." *arXiv*
615 *preprint arXiv:1901.03407*.
- 616 Chandola, V., A. Banerjee, and V. Kumar. 2009. "Anomaly Detection: A Survey." *ACM*
617 *Computing Surveys (CSUR)* 41 (15): 1-58. doi:<https://doi.org/10.1145/1541880.1541882>.
- 618 Chen, H., A.K. Githeko, G. Zhou, J.I. Githure, and G. Yan. 2006. "New records of *Anopheles*
619 *arabiensis* breeding on the Mount Kenya highlands indicate indigenous malaria
620 transmission." *Malaria Journal* 5 (17). doi:<https://doi.org/10.1186/1475-2875-5-17>.
- 621 Connolly-Boutin, L., and B. Smit. 2016. "Climate change, food security, and livelihoods in Sub-
622 Saharan." *Regional Environmental Change* 16: 385 - 399.
623 doi:<https://doi.org/10.1007/s10113-015-0761-x>.
- 624 Das, M., and S. Parthasarathy. 2009. "Anomaly detection and spatio-temporal analysis of global
625 climate system." *Proceedings of the third international workshop on knowledge discovery*
626 *from sensor data*. Paris: Association for Computing Machinery. 142-150.
627 doi:<https://doi.org/10.1145/1601966.1601989>.
- 628 Deo, R.C., and M. Sahin. 2015. "Application of the artificial neural network model for prediction
629 of monthly standardised precipitation and evapotranspiration index using
630 hydrometeorological parameters and climate indices in eastern Australia." *Atmospheric*
631 *Research* 161–162: 65 - 81. doi:<https://doi.org/10.1016/j.atmosres.2015.03.018>.
- 632 Dercon, S., R. V. Hill, D. Clarke, I. Outes-Leon, and A. S. Taffesse. 2014. "Offering rainfall
633 insurance to informal insurance groups: Evidence from a field experiment in Ethiopia."
634 *Journal of Development Economics* 106: 132-143.
635 doi:<https://doi.org/10.1016/j.jdeveco.2013.09.006>.
- 636 Food and Agriculture Organization (FAO). 2009. "FAO: Technical papers from the Expert
637 Meeting on How to Feed the World in 2050." November 11. Accessed September 8, 2021.
638 <http://www.fao.org/wsfs/forum2050/wsfs-forum/en/on>.
- 639 Fung, K., Y. Huang, C. Koo, and Y. Soh. 2020. "Drought forecasting: A review of modelling
640 approaches 2007-2017." *Journal of Water and Climate Change* 11 (3): 771-799.
641 doi:<https://doi.org/10.2166/wcc.2019.236>.
- 642 Goedde, L., A. Ooko - Ombaka, and G. Pais. 2019. *Winning in Africa's agricultural market*.
643 McKinsey and Company. February 19. Accessed September 8, 2021.
644 [https://www.mckinsey.com/industries/agriculture/our-insights/winning-in-africas-](https://www.mckinsey.com/industries/agriculture/our-insights/winning-in-africas-agricultural-market)
645 [agricultural-market](https://www.mckinsey.com/industries/agriculture/our-insights/winning-in-africas-agricultural-market).
- 646 Goldstein, M., and A. Dengel. 2012. "Histogram-based outlier score (HBOS): A fast unsupervised
647 anomaly detection algorithm." *35th German Conference on Artificial Intelligence (KI-*
648 *2012)*. Germany. 59-63.

- 649 Hakala, K., N. Addor, C. Teutschbein, M. Vis, H. Dakhlaoui, and J. Seibert. 2019. "Hydrological
650 Modeling of Climate Change Impacts." In *Encyclopedia of Water: Science, Technology,*
651 *and Society*, 1-20. John Wiley & Sons.
652 doi:https://doi.org/10.1002/9781119300762.wsts0062.
- 653 Hanel, M., O. Rakovec, Y. Markonis, P. Máca, L. Samaniego, J. Kyselý, and R. Kumar. 2018.
654 "Revisiting the recent European droughts from a long-term perspective." *Scientific Reports*
655 8 (1): 9499. doi:https://doi.org/10.1038/s41598-018-27464-4.
- 656 Hannah, L. 2015. "The Climate System and Climate Change." In *Climate Change Biology (Second*
657 *Edition)*. Cambridge, MA: Academic Press.
- 658 Hargreaves, G. H., and Z. A. Samani. 1985. "Reference crop evapotranspiration from
659 temperature." *Applied Engineering in Agriculture* 1 (2): 96-99.
660 doi:https://doi.org/10.13031/2013.26773.
- 661 Hazell, P., and S. Wood. 2008. "Drivers of change in global agriculture." *Philosophical*
662 *Transactions of the Royal Society B: Biological Sciences* 363 (1491): 495-515.
663 doi:https://doi.org/10.1098/rstb.2007.2166.
- 664 He, Z., X. Xu, and S. Deng. 2003. "Discovering cluster-based local outliers." *Pattern Recognition*
665 *Letters* 24 (9-10): 1641 - 1650. doi:https://doi.org/10.1016/S0167-8655(03)00003-5.
- 666 Inoubli, R., A. B. Abbes, I. R. Farah, V. Singh, T. Tadesse, and M. T. Sattari. 2020. "A review of
667 drought monitoring using remote sensing and data mining methods." *5th International*
668 *Conference on Advanced Technologies for Signal and Image Processing (ATSIP) 2020*.
669 Tunisia: IEEE. doi:https://doi.org/10.1109/ATSIP49331.2020.9231697.
- 670 Juma, B., L. O. Olang, M. Hassan, S. Chasia, V. Bukachi, P. Shiundu, and J. Mulligan. 2020.
671 "Analysis of rainfall extremes in the Ngong River Basin of Kenya: Towards integrated
672 urban flood risk management." *Physics and Chemistry of the Earth, Parts A/B/C* 102929.
673 doi:https://doi.org/10.1016/j.pce.2020.102929.
- 674 Kebede, A., A. Hasen, and W. Negatu. 2011. "A comparative analysis of vulnerability of
675 pastoralists and agro-pastoralists to climatechange: A case study in Yabello Woreda of
676 Oromia Region, Ethiopia." *Ethiopian Journal of Development Research* 33 (1): 61-95.
677 doi:https://doi.org/10.4314/ejdr.v32i2.68611.
- 678 Kenya Insurance Regulatory Authority. 2015. "The Kenya Index-Based Insurance." June 12.
679 Accessed September 20, 2021.
680 https://www.ira.go.ke/images/docs/THE_DRAFT_KENYA_INDEX_BASED_INSURA
681 NCE_POLICY_PAPER_2015.pdf.
- 682 Kundzewicz, Z.W., S. Kanae, S.I. Seneviratne, J. Handmer, N. Nicholls, P. Peduzzi, R. Mechler,
683 et al. 2014. "Flood risk and climate change: Global and regional perspectives."
684 *Hydrological Sciences Journal* 59 (1): 1-28.
685 doi:https://doi.org/10.1080/02626667.2013.857411.

- 686 Liu, F. T., K. M. Ting, and Z. H. Zhou. 2012. "Isolation-based anomaly detection." *ACM*
687 *Transactions on Knowledge Discovery from Data (TKDD)*. 6 (1): 1-39.
688 doi:<https://doi.org/10.1145/2133360.2133363>.
- 689 Luhunga, P., J. Botai, and F. Kahimba. 2016. "Evaluation of the performance of CORDEX
690 regional climate models in simulating present climate conditions of Tanzania." *Journal of*
691 *Southern Hemisphere Earth Systems Science* 66 (1): 32-54.
692 doi:<https://doi.org/10.22499/3.6601.005>.
- 693 Madadgar, S., A. AghaKouchak, S. Shukla, A. W. Wood, L. Cheng, K. L. Hsu, and M. Svoboda.
694 2016. "A hybrid statistical-dynamical framework for meteorological drought prediction:
695 Application to the southwestern United States." *Water Resources Research* 52 (7): 5095-
696 5110. doi:<https://doi.org/10.1002/2015WR018547>.
- 697 Maidment, R., E. Black, and M. Young. 2017. "TAMSAT Daily Rainfall Estimates (Version 3.0)."
698 *Dataset*. University of Reading. Accessed September 9, 2021.
699 doi:<https://doi.org/10.17864/1947.112>.
- 700 Makena, B., M. Osunga, S. Kingori, and H.S. Abdillahi. 2021. *An Application of Flood Risk*
701 *Analysis for Impact Based Forecasting in Kenya*. Nairobi, Kenya: International Center for
702 Humanitarian Affairs and Kenya Red Cross.
- 703 McKee, T. B., N. J. Doesken, and J. Kleist. 1993. "The relationship of drought frequency and
704 duration to time scales." *In Proceedings of the 8th Conference on Applied Climatology* 17
705 (22): 179-183.
- 706 Meier, H. M., A. Höglund, R. Döscher, H. Andersson, U. Löptien, and E. Kjellström. 2011.
707 "Quality assessment of atmospheric surface fields over the Baltic Sea from an ensemble of
708 regional climate model simulations with respect to ocean dynamics." *Oceanologia* 53: 193-
709 227. doi:<https://doi.org/10.5697/oc.53-1-TI.193>.
- 710 Mendoza, P. A., M. P. Clark, N. Mizukami, A. J. Newman, M. Barlage, E. D. Gutmann, R.M.
711 Rasmussen, B. Rajogopalan, L.M. Brekke, and J. R. Arnold. 2015. "Effects of hydrologic
712 model choice and calibration on the portrayal of climate change impacts." *Journal of*
713 *Hydrometeorology* 16 (2): 762-780. doi:<https://doi.org/10.1175/JHM-D-14-0104.1>.
- 714 Min, E., W. Hazeleger, G. J. Van Oldenborgh, and A. Sterl. 2013. "Evaluation of trends in high
715 temperature extremes in north-western Europe in regional climate models." *Environmental*
716 *Research Letters* 8 (1): 014011. doi:<https://doi.org/10.1088/1748-9326/8/1/014011>.
- 717 Mirza, M. M. Q. 2003. "Climate change and extreme weather events: Can developing countries
718 adapt?" *Climate Policy* 3 (3): 233-248. doi:[https://doi.org/10.1016/S1469-3062\(03\)00052-](https://doi.org/10.1016/S1469-3062(03)00052-4)
719 4.
- 720 Mizra, M.M.Q., and A.U. Ahmed. 2010. "Global Environmental Changes in South Asia." In *A*
721 *Review on Current Status of flood and drought forecasting in South Asia.*, edited by A.P.
722 Mitra and C. Sharma, 233-243. Dodrecht: Springer. doi:[https://doi.org/10.1007/978-1-](https://doi.org/10.1007/978-1-4020-9913-7)
723 4020-9913-7.

- 724 Mizukami, N., Martyn P. Clark, Ethan D. Gutmann, Pablo A. Mendoza, Andrew J. Newman, Bart
725 Nijssen, B. Livneh, L.E. Hay, J.R. Arnold, and L. D. Brekke. 2016. "Implications of the
726 methodological choices for hydrologic portrayals of climate change over the contiguous
727 United States: Statistically downscaled forcing data and hydrologic models." *Journal of*
728 *Hydrometeorology* 17 (1): 73-98. doi:<https://doi.org/10.1175/JHM-D-14-0187.1>.
- 729 Muller, C., W. Cramer, W.L. Hare, and H. Lotze-Campen. 2011. "Climate change risks for African
730 agriculture." Edited by Robert W. Kates. *Proceedings of the National Academy of Sciences*.
731 4313-4315. doi:<https://doi.org/10.1073/pnas.1015078108>.
- 732 Mumo, L., and J. Yu. 2020. "Gauging the performance of CMIP5 historical simulation in
733 reproducing observed gauge rainfall over Kenya." *Atmospheric Research* 236: 104808.
734 doi:<https://doi.org/10.1016/j.atmosres.2019.104808>.
- 735 Mutsotso, R. B., A. W. Sichangi, and G. O. Makokha. 2018. "Spatio-temporal drought
736 characterization in Kenya from 1987 to 2016." *Advances in Remote Sensing* 7 (2): 125.
737 doi:<https://doi.org/10.4236/ars.2018.72009>.
- 738 National Drought Management Authority. 2020. *Turukana County Drought Early Warning*
739 *Bulletin for December 2020*. OCHA Services, Relief Web. December. Accessed
740 September 12, 2021. [https://reliefweb.int/report/kenya/turkana-county-drought-early-](https://reliefweb.int/report/kenya/turkana-county-drought-early-warning-bulletin-december-2020)
741 [warning-bulletin-december-2020](https://reliefweb.int/report/kenya/turkana-county-drought-early-warning-bulletin-december-2020).
- 742 National Management Authority. 2020. *Wajir County: Drought Early Warning Bulletin for*
743 *December 2020*. OCHA Services, Relief Web. December. Accessed September 12, 2021.
744 [https://reliefweb.int/report/kenya/wajir-county-drought-early-warning-bulletin-december-](https://reliefweb.int/report/kenya/wajir-county-drought-early-warning-bulletin-december-2020)
745 [2020](https://reliefweb.int/report/kenya/wajir-county-drought-early-warning-bulletin-december-2020).
- 746 Niang, I., O.C. Ruppel, M.A. Abdrabo, A. Essel, C. Lennard, J. Padgham, and P. Urquhart. 2014.
747 "Climate Change 2014: Impacts, Adaptation, and Vulnerability. Part B: Regional Aspects.
748 Contribution of Working Group II to the Fifth Assessment Report of the Intergovernmental
749 Panel on Climate Change." 1199-1265. Cambridge: Cambridge University Press.
- 750 Opere, A. 2013. "Floods in Kenya." *Developments in Earth Surface Processes* (Elsevier) 16: 315-
751 330. doi:<https://doi.org/10.1016/B978-0-444-59559-1.00021-9>.
- 752 Osbahr, H., C. Twyman, N. Adger, and D.S.G. Thomas. 2008. "Effective livelihood adaptation to
753 climate change disturbance: Scale dimensions of practice in Mozambique." *Geoforum* 39
754 (6): 1951-1964. doi:<https://doi.org/10.1016/j.geoforum.2008.07.010>.
- 755 Owuor, P. 2015. "The disaster profile of Kenya." Unit for Research in Emergency and Disaster,
756 University of Oviedo, Spain, 1-45.
- 757 Pfister, S., P. Bayer, A. Koehler, and S. Hellweg. 2011. "Projected water consumption in future
758 global agriculture: Scenarios and related impacts." *Science of the Total Environment* 409
759 (20): 4206–4216. doi:<https://doi.org/10.1016/j.scitotenv.2011.07.019>.

- 760 Reich, P.F., S.T. Numben, R. Almaraz, and H. Eswaran. 2001. "Land resources stresses and
761 desertification in Africa." *Agro-Science* 2 (2): 1-10.
762 doi:<https://doi.org/10.4314/as.v2i2.1484>.
- 763 Richard, Y., N. Fauchereau, I. Pocard, M. Rouault, and S. Trzaska. 2001. "20th century droughts
764 in southern Africa: spatial and temporal variability, teleconnections with oceanic and
765 atmospheric conditions." *International Journal of Climatology: A Journal of the Royal
766 Meteorological Society* 21 (7): 873 – 885. doi:<https://doi.org/10.1002/joc.656>.
- 767 Ringler, C., T. Zhu, X. Cai, J. Koo, and D. Wang. 2010. *Climate change impacts on food security
768 in sub-Saharan Africa. Insights from Comprehensive Climate Change Scenarios*.
769 International Food Policy Research Institute, Washington, D.C.: International Food Policy
770 Research Institute (IFPRI), 28.
- 771 Sarr, B. 2012. "Present and future climate change in the semi-arid region of West Africa: A crucial
772 input for practical adaptation in agriculture." *Atmospheric Science Letters* 13 (2): 108-112.
773 doi:<https://doi.org/10.1002/asl.368>.
- 774 Slater, L. J., and G. Villarini. 2018. "Enhancing the predictability of seasonal streamflow with a
775 statistical-dynamical approach." *Geophysical Research Letters* 45 (13): 6504-6513.
776 doi:<https://doi.org/10.1029/2018GL077945>.
- 777 Songok, C.K., E.C. Kipkorir, and E.M. Mugalavai. 2011. "Integration of Indigenous Knowledge
778 Systems into Climate Change Adaptation and Enhancing Food Security in Nandi and
779 Keiyo Districts, Kenya." In *Experiences of Climate Change Adaptation in Africa. Climate
780 Change Management*, edited by Filho W. Leal, 69-95. Hamburg, Berlin: Springer.
781 doi:https://doi.org/10.1007/978-3-642-22315-0_5.
- 782 Songok, C.K., E.C. Kipkorir, E.M. Mugalavai, A.C. Kwonyike, and C. Ngweno. 2011. "Improving
783 the Participation of Agro-Pastoralists in Climate Change Adaptation and Disaster Risk
784 Reduction Policy Formulation: A Case Study from Keiyo District, Kenya." In *Experiences
785 of Climate Change Adaptation in Africa. Climate Change Management.*, edited by Filho
786 W. Leal, 55–68. Hamburg, Berlin: Springer. doi:[https://doi.org/10.1007/978-3-642-22315-
787 0_4](https://doi.org/10.1007/978-3-642-22315-0_4).
- 788 Thomas, D.S.G., C. Twyman, H. Osbahr, and B. Hewitson. 2007. "Adaptation to climate change
789 and variability: Farmer responses to intraseasonal precipitation trends in South Africa."
790 *Climatic Change* 83 (3): 301 - 322. doi:<https://doi.org/10.1007/s10584-006-9205-4>.
- 791 Thompson, J., and I. Scoones. 2009. "Addressing the dynamics of agri-food systems: An emerging
792 agenda for social science research." *Environmental Science & Policy* 12 (4): 386-397.
793 doi:<https://doi.org/10.1016/j.envsci.2009.03.001>.
- 794 Tschakert, P., R. Sagoe, G. Ofori-Darko, and S.N. Codjoe. 2010. "Floods in the Sahel: An analysis
795 of anomalies, memory, and anticipatory learning." *Climatic Change* 103 (3): 471-502.
796 doi:<https://doi.org/10.1007/s10584-009-9776-y>.

- 797 Vicente-Serrano, S. M., S. Beguería, and J. I. López-Moreno. 2010. "A multiscale drought index
798 sensitive to global warming: The standardized precipitation evapotranspiration index."
799 *Journal of Climate* 23 (7): 1696-1718. doi:<https://doi.org/10.1175/2009JCLI2909.1>.
- 800 Wairimu, E., G. Obare, and M. Odendo. 2016. "Factors affecting weather index-based crop
801 insurance in Laikipia County, Kenya." *Journal of Agricultural Extension and Rural*
802 *Development* 8 (7): 111-121. doi:<https://doi.org/10.5897/JAERD2016.0769>.
- 803 Wasko, C., and R. Nathan. 2019. "Influence of changes in rainfall and soil moisture on trends in
804 flooding." *Journal of Hydrology* 575: 432 - 441.
805 doi:<https://doi.org/10.1016/j.jhydrol.2019.05.054>.
- 806 Wibisono, S., M. Anwar, A. Supriyanto, and I. Amin. 2021. "Multivariate weather anomaly
807 detection using DBSCAN clustering algorithm." *Journal of Physics: Conference Series*
808 (IOP Publishing) 1869 (1). doi:<https://doi.org/10.1088/1742-6596/1869/1/012077>.
- 809 Wilby, R. L. 2010. "Evaluating climate model outputs for hydrological applications."
810 *Hydrological Sciences Journal* 55 (7): 1090-1093.
811 doi:<https://doi.org/10.1080/02626667.2010.513212>.
- 812 Wlokas, H.L. 2008. "The impacts of climate change on food security and health in Southern
813 Africa." *Journal of Energy in Southern Africa* 19 (4): 12-20.
- 814 Woodhouse, C. A., G. T. Pederson, K. Morino, S. A. McAfee, and G. J. McCabe. 2016. "Increasing
815 influence of air temperature on upper Colorado River streamflow." *Geophysical Research*
816 *Letters* 43 (5): 2174-2181. doi:<https://doi.org/10.1002/2015GL067613>.
- 817

818 Statements and Declarations

819 Funding

820 The research detailed in the submitted paper was made possible by a grant (Grant No. 109675-
821 001/002) from the International Development Research Centre (IDRC).

822 Competing Interests

823 The authors have no relevant financial or non-financial interests to disclose.

824 Author's Contribution

825 Dr. Angeline Wairegi and Dr. John Olukuru provided guidance on the study conceptualization,
826 design, and execution. Material preparation, data collection and analysis were performed by Alvin
827 M. Igobwa and Jeremy Gachanja. The manuscript was written by Dr. Angeline Wairegi and Betsy
828 Muriithi. Dr. Angeline Wairegi, Dr. John Olukur, Alvin M. Igobwa, Jeremy Gachanja, Betsy
829 Muriithi, and Dr. Isaac Rutenberg were involved in reviewing and editing of the manuscript, and
830 approved the final manuscript.

831 Data Availability

832 The datasets generated and analysed during the current study are available on the Zenodo platform,
833 DOI 10.5281/zenodo.5730074, [<https://zenodo.org/record/5730074#.YgOeSN9BzIU>].

834

835 Ethical Approval

836 Not Applicable

837 Consent to Participate

838 Not Applicable

839 Consent to Publish

840 All authors listed above consent to have the submitted manuscript published in the Climate Change
841 journal.